

Catalytic production of *Jatropha* biodiesel and hydrogen with magnetic carbonaceous acid and base synthesized from *Jatropha* hulls



Fan Zhang^{a,e,*}, Xiao-Fei Tian^{b,a,*}, Zhen Fang^{c,a,*}, Mazloom Shah^{a,d}, Yi-Tong Wang^{a,e}, Wen Jiang^a, Min Yao^a

^a Chinese Academy of Sciences, Biomass Group, Key Laboratory of Tropical Plant Resources and Sustainable Use, Xishuangbanna Tropical Botanical Garden, 88 Xuefulu, Kunming, Yunnan 650223, China

^b School of Bioscience and Bioengineering, South China University of Technology, University Mega Centre, Guangzhou, Guangdong 510006, China

^c Biomass Group, College of Engineering, Nanjing Agricultural University, 40 Dianjiangtai Road, Nanjing, Jiangsu 210031, China

^d Department of Chemistry, Women University of Azad Jammu and Kashmir, Bagh 12500, Pakistan

^e University of Chinese Academy of Sciences, 19A Yuquan Road, Beijing 100049, China

ARTICLE INFO

Article history:

Received 21 December 2016

Received in revised form 20 February 2017

Accepted 8 March 2017

Available online 21 March 2017

Keywords:

Jatropha oil

Hulls

Magnetic catalyst

Biodiesel

Hydrothermal gasification

ABSTRACT

Magnetic carbonaceous solid acid (C-SO₃H@Fe/JHC) and base (Na₂SiO₃@Ni/JRC) catalysts were synthesized by loading active groups on the carbonaceous supporters derived from *Jatropha*-hull hydrolysate and hydrolysis residue. Characterization of their morphology, magnetic saturation, functional groups and total acid/base contents were performed by various techniques. Additional acidic functional groups that formed with *Jatropha*-hull hydrolysate contributed to the high acidity of C-SO₃H@Fe/JHC catalyst for the pretreatment (esterification) of crude *Jatropha* oil with high acid values (AV). The AV of esterified *Jatropha* oil dropped down from 17.2 to 1.3 mg KOH/g, achieving a high biodiesel yield of 96.7% after subsequent transesterification reaction with Na₂SiO₃@Ni/JRC base that was cycled at least 3 times with little loss of catalysis activity. Both solid acid and base catalysts were easily recovered by magnetic force with average recovery yields of 90.3 wt% and 86.7%, respectively. After washed by ethanol, the catalysts were cycled for 10 times. The AV of esterified oil and biodiesel yield using the recycled catalysts remained below 2.0 mg KOH/g and above 85%, respectively. The existence of catalyst ions and residual methanol contributed to high H₂ yield (81.0%) and high purity (81.7%) in the hydrothermal gasification of glycerol by-product using the deactivated solid base.

© 2017 Elsevier Ltd. All rights reserved.

1. Introduction

As more and more intensive oil supply and the serious pollution of vehicle emissions [1,2], biodiesel (fatty acids methyl esters, FAMES) [3], ethanol [4], and hydrogen [5] have become the focus of development of renewable and clean transportation fuels. Biodiesel is produced with high yield through the transesterification of triglycerides with bases including homogenous catalysts of potassium and sodium methoxides [6], and heterogeneous catalysts such as CaO-MoO₃-SBA-15 [7], CaO [8] and re-crystallized hydrothermalite [9]. However, low free fatty acids (FFAs) are required

for crude oils for transesterification to avoid saponification with these catalysts [10]. For biodiesel production from crude oils with high FFAs or high acid values (AV), solid acid catalysts such as Nafion [11], supported heteropolyacid [12], and carbon nanotube-based solid sulfonic acids [13] were directly applied while higher reaction temperatures and longer time were required [14,15]. Alternatively, a two-step biodiesel production method was developed, in which high FFAs in crude oils could be firstly esterified catalyzed by acids followed by transesterification of the oils catalyzed by base catalysts [16,17]. Heterogeneous catalysis of the two-step biodiesel production became a popular technique with significant advantages of high biodiesel yield and easiness for catalyst recycles [18].

The recovery of solid catalysts was usually performed by filtration or centrifugation methods that were time-consuming with low energy efficiency [15]. The development of magnetic solid catalysts would benefit the easiness of catalyst separation by a magnet attraction. Magnetic carbonaceous solid acid (Fe/C-SO₃H) was successfully applied in the esterification of oleic acid [19].

* Corresponding authors at: Biomass Group, College of Engineering, Nanjing Agricultural University, 40 Dianjiangtai Road, Nanjing, China (Z. Fang). Key Laboratory of Tropical Plant Resources and Sustainable Use, Xishuangbanna Tropical Botanical Garden, Chinese Academy of Sciences, Kunming, China (F. Zhang). School of Bioscience and Bioengineering, South China University of Technology, Guangzhou, China (X.F. Tian).

E-mail addresses: zhangfan@xtbg.ac.cn (F. Zhang), xtien@scut.edu.cn (X.-F. Tian), zhenfang@njau.edu.cn (Z. Fang).

URL: <http://biomass-group.njau.edu.cn/> (Z. Fang).

Magnetic carbonaceous solid base ($\text{Na}_2\text{SiO}_3@\text{Fe}_3\text{O}_4/\text{C}$) also possessed high activities in catalyzing transesterification reactions in biodiesel production [10]. $\text{Na}_2\text{SiO}_3@\text{Fe}_3\text{O}_4/\text{C}$ catalyst after five cycles could still achieve a 1.8-times recovery rate as that using sole Na_2SiO_3 particles (96.1 vs. 54.4 wt%) [10,20] due to the high separation efficiency by a magnet. Although these magnetic solid catalysts showed promising advantages in biodiesel production, source of their carbonaceous supporters were from expensive edible sugars or commercial active carbons [10,19]. Any potential application of the reported $\text{Na}_2\text{SiO}_3@\text{Fe}_3\text{O}_4/\text{C}$ catalyst for H_2 production was not possible due to the lack of necessary active elements such as Ni [10,21].

The drought-resistant perennial *Jatropha* trees grow well in marginal/poor soils [22]. *Jatropha* oil has attracted great attention as a promising crude oil resource for biodiesel production [23]. By 2008, the global plantation of *Jatropha* trees has reached about 9.0×10^6 ha in Asia, Africa and Latin America [24] including about 1.5×10^5 ha in China [23]. The state forestry administration of China declared to expand the *Jatropha* tree plantation (including natural forests) to 1.45×10^7 ha in southwest of China until 2020 [25]. As reported [26], producing 1000 L of *Jatropha* oil could generate 6.86 t *Jatropha*-hull waste. After transesterification, the reaction mixture contained approximately 10 wt% by-product glycerol [27]. With a growth of *Jatropha* biodiesel production, large quantities of *Jatropha*-hulls and glycerol will be generated. It is important to make full use of these *Jatropha* wastes.

In this study, magnetic carbonaceous solid acid and base catalysts were synthesized by loading active groups on the carbonaceous supporters derived from *Jatropha*-hull hydrolysate and hydrolysis residue. They were applied in the two-step biodiesel production with high-AV *Jatropha* oil as feedstock. The crude glycerol generated from biodiesel production was further hydrothermally gasified for H_2 production that was catalyzed by the deactivated base catalyst.

2. Experimental

2.1. Material

Jatropha-hull powders (48.6 C, 7.23 H and 41.1 O, wt%; particle size <200 μm) were provided by Yunnan Shenyu New Energy Co., Ltd. (Chuxiong, Yunnan). Crude *Jatropha* oil (AV of 17.2 mg KOH/g, molecular weight of 942.9 g/mol, Scheme 1a) was supplied by Xishuangbanna Tropical Botanical Garden (Mengla, Yunnan). $\text{FeCl}_3 \cdot 6\text{H}_2\text{O}$ ($\geq 99.0\%$), $\text{Ca}(\text{OH})_2$ ($\geq 95.0\%$), H_2SO_4 ($\geq 98.0\%$), $\text{Ni}(\text{NO}_3)_2 \cdot 6\text{H}_2\text{O}$ ($\geq 98.0\%$), solid urea ($\geq 95.0\%$), $\text{Na}_2\text{SiO}_3 \cdot 9\text{H}_2\text{O}$ (19.3–22.8 wt% Na_2O , weight ratio of $\text{Na}_2\text{O}/\text{SiO}_2 = 1.03 \pm 0.03$), methanol ($\geq 99.5\%$), potassium phthalate monoacid [FtHK, 99.5%], KOH ($\geq 85.0\%$), CH_2Cl_2 ($\geq 99.5\%$), ethanol ($\geq 99.5\%$) and phenothalin were provided by Xilong Chemical Factory Co., Ltd. (Shantou, Guangdong). Standard heptadecanoic acid methyl ester ($\text{C}_{17:0}$), other methyl esters [palmitate ($\text{C}_{16:0}$), palmitoleate ($\text{C}_{16:1}$), stearate ($\text{C}_{18:0}$), oleate ($\text{C}_{18:1}$), linoleate ($\text{C}_{18:2}$) and linolenate ($\text{C}_{18:3}$), $\geq 99.0\%$], NaHCO_3 (99.7%), Na_2CO_3 ($\geq 99.99\%$), NaOH (99.99%), Na_2SO_4 (99.99%) and HCl (0.05 M, 99.0%) were purchased from Sigma–Aldrich (Shanghai).

2.2. Preparation of *Jatropha*-hull hydrolysate and residue

Jatropha-hull hydrolysate was prepared in a 500-mL ZrO_2 -coated autoclave (FCFD03-50, Jianbang Chemical Mechanical Co. Ltd., Yantai, Shandong) containing 15 g *Jatropha* hulls, 200 mL H_2O and 6 g concentrated H_2SO_4 (98%, w/w). The hydrolysis was performed at 150 °C for 1.5 h with a stirring speed of 300 rpm.

After reaction, the solid residue was collected by filtration through a filter (RW19, pore size of 1.2 μm , Merck Millipore Ltd., Cork, Ireland). The hydrolysate was neutralized with saturated $\text{Ca}(\text{OH})_2$ solution and concentrated through vacuum evaporation at 65 °C until reaching the total organic carbon (TOC) of 61 g/L. The collected solid residue was washed twice with hot distilled water (80 °C) and dried at 75 °C until reaching a constant weight. The dried *Jatropha* hull hydrolysis residue (JR) was sieved through a 200-mesh (particle size $\leq 75 \mu\text{m}$) before use.

2.3. Catalyst preparation

2.3.1. Magnetic carbonaceous acid ($\text{C}-\text{SO}_3\text{H}@\text{Fe}/\text{JHC}$)

Solid acid was synthesized by a 3-step method (Scheme 2) based on the previous study [14]. Firstly (Scheme 2i), $\text{FeCl}_3 \cdot 6\text{H}_2\text{O}$ (81.1 g), solid urea (30.0 g) and *Jatropha*-hull hydrolysate (0.3 L) were mixed in the autoclave and heated to 180 °C within 36 min. The reaction was conducted for 14 h with a stirring speed of 500 rpm. After reaction, the solid residual produced from the hydrolysate polymerization and iron precipitation [$\text{CO}(\text{NH}_2)_2 + \text{H}_2\text{O} \rightarrow \text{NH}_3\uparrow + \text{CO}_2\uparrow + \text{NH}_4\text{OH}$; $\text{FeCl}_3 + \text{NH}_4\text{OH} \rightarrow \text{Fe}(\text{OH})_3\downarrow + \text{NH}_4\text{Cl}$] was separated from the reaction mixture and washed with deionized water and ethanol for several times until reaching neutral. After freeze-dried at -47 °C for 24 h, the residual was submitted in a tubular furnace for pyrolysis at 700 °C (with heating rate of 7.4 °C/min) for 1.5 h. N_2 was used as the protect gas with a flowing rate of 200 mL/min. During the pyrolysis, the magnetic core (Fe/JHC) was formed through dehydration and reduction reactions [$\text{Fe}(\text{OH})_3 \rightarrow \text{Fe}_2\text{O}_3 + \text{H}_2\text{O}$; $\text{Fe}_2\text{O}_3 + \text{C} \rightarrow \text{Fe}_3\text{O}_4/\text{Fe} + \text{CO}/\text{CO}_2\uparrow$].

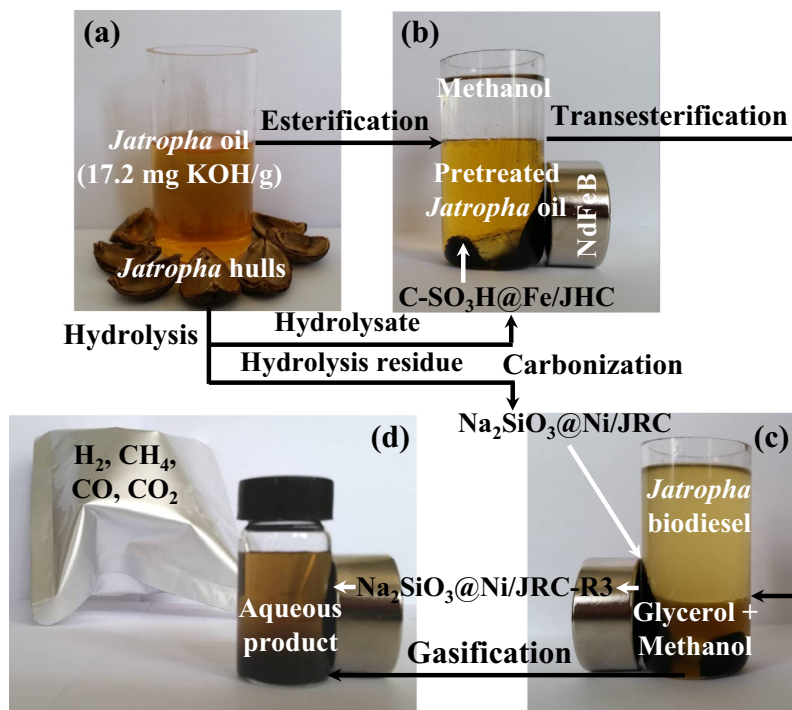
Because the dissolution of $\text{Fe}_3\text{O}_4/\text{Fe}$ in H_2SO_4 [14] led to an extremely weak magnetism (0.56 Am^2/kg) after sulfonation, pre-coating of carbon layers on the magnetic core was performed with the *Jatropha*-hull hydrolysate (Scheme 2ii). Fe/JHC powders (20 g) were dispersed in *Jatropha*-hull hydrolysate (0.3 L). The mixture was incubated at 180 °C for 14 h with a stirring speed of 500 rpm. After reaction, the coated magnetic carbon ($\text{C}@\text{Fe}/\text{JHC}$) was collected by a magnet and washed with deionized water and ethanol. The carbon coating was stabilized through pyrolysis at 600 °C (heating rate of 6.3 °C/min) for 1.5 h.

In the sulfonation (Scheme 2iii), a 500-mL three-neck flask containing 10 g $\text{C}@\text{Fe}/\text{JHC}$ particles and 200 mL concentrated H_2SO_4 (98%, w/w) was incubated at 150 °C for 16 h with a nitrogen flow rate of 100 mL/min. After washed with hot distilled water (80 °C), the solid acid catalyst ($\text{C}-\text{SO}_3\text{H}@\text{Fe}/\text{JHC}$) was obtained, freeze-dried and screened through a 200-mesh sieve for the esterification of *Jatropha* oil.

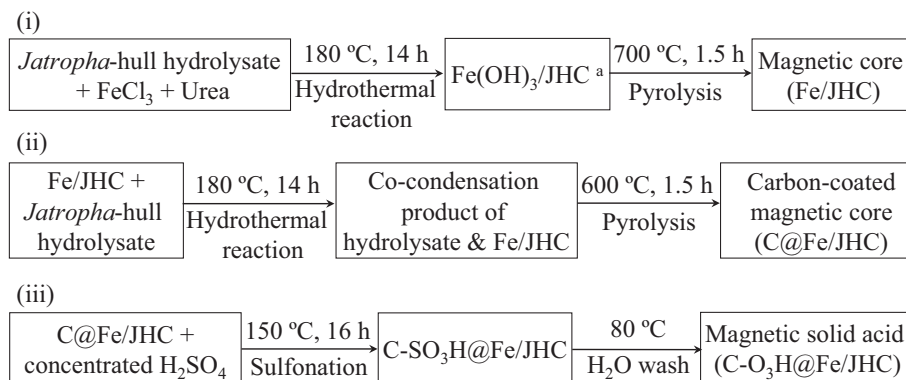
2.3.2. Magnetic solid base ($\text{Na}_2\text{SiO}_3@\text{Ni}/\text{JRC}$)

A 500 mL reaction solution containing 145.5 g $\text{Ni}(\text{NO}_3)_2 \cdot 6\text{H}_2\text{O}$, 60 g solid urea and 24 g *Jatropha* residue (JR) was loaded in a 1-L three-neck flask equipped with a condenser. The flask was incubated at 135 °C in oil bath for 10 h with a stirring speed at 500 rpm. After reaction, the solid product with $\text{Ni}(\text{OH})_2$ precipitate was collected by filtration (1.2 μm) and washed with deionized water. For the synthesis of Ni/JRC (JRC : *Jatropha* residue carbon) supporter, the solid product was submitted to calcination at 700 °C for 2 h with a nitrogen flow rate of 200 mL/min.

Ni/JRC supporter (20 g) and $\text{Na}_2\text{SiO}_3 \cdot 9\text{H}_2\text{O}$ (120 g) were loaded in a 1-L flask containing 150 mL water. The solution was stirred and evaporated at 85 °C to form a gel. Followed by calcination at 400 °C for 2 h, the solid was processed by ball milling with ZrO_2 balls for 12 h at a spinning speed of 230 rpm and screened through a 200-mesh sieve. The prepared $\text{Na}_2\text{SiO}_3@\text{Ni}/\text{JRC}$ base contained 72.0 wt% Na_2SiO_3 .



Scheme 1. A workflow for the production of biodiesel and H₂ (a) raw materials, (b) esterified *Jatropha* oil, (c) biodiesel and by-products, and (d) hydrothermally gasified products [magnetic carbonaceous solid acid (C-SO₃H@Fe/JHC) and base (Na₂SiO₃@Ni/JRC) derived from *Jatropha* hulls].



Scheme 2. Preparation of the magnetic solid acid through combination of hydrothermal precipitation and pyrolysis (i and ii), as well as sulfonation (iii). ^aJHC: *Jatropha* hull carbon.

2.4. Instrumentation

The crystal forms, magnitude of magnetism, morphologies and total acid/base contents of the synthesized supporters/catalysts were characterized by X-ray diffraction (XRD, Rigaku Rotaflex RAD-C, Tokyo with Cu K α radiation source), vibrating sample magnetometer (VSM; lakeshore7407, Lake Shore Cryotronics, Inc., Westerville, OH), scanning electron microscope (SEM; ZEISS EVO LS10, Cambridge, UK) and temperature programmed desorption (TPD; Chemisorption analyzer, Quantachrome Instruments, Boynton Beach, FL), respectively. Specific surface area and pore volume were determined by Bruner Emmett and Teller (BET) method (Tristar II 3020, Micromeritics Instrument Co., Ltd., Northcross, GA). Chemical bonds were analyzed by Fourier transform-infrared spectroscopy (FT-IR; Nicolet iS10, Thermo Fisher Scientific Co., Ltd., Waltham, MA) from 4000 to 400 cm⁻¹ with the resolution of 0.4–4 cm⁻¹. Inorganic compositions contained in crude glycerol and catalysts were determined using inductively coupled

plasma-optical emission spectrometry (ICP-OES; Optima 5300 DV, Perkin-Elmer Inc., Waltham, MA). Before ICP analysis, catalysts and crude glycerol were dissolved in concentrated HCl.

Contents of acidic groups on the derived carbonaceous supporters were determined according to the modified acid-base titration method using phenolphthalein as an indicator [28,29]. Each 0.50 g sample was mixed with 25.0 mL of (a) NaHCO₃ (0.05 M, 99.7%), (b) Na₂CO₃ (0.05 M, 99.99%), (c) NaOH (0.05 M, 99.99%) and (d) Na₂SO₄ (0.1 M, 99.99%) for acid groups (a. carboxylic, b. phenols, c. lactones groups and d. sulfonic group) with stirring for 24 h, respectively [28,29]. The extracted solutions (a–c) after filtration were acidified by 10–15 mL HCl (0.05 M, 99.0%), placed in a sealed tube, and bubbled with nitrogen for 2 h at 80 °C for 30 min. The acid group contents (carboxylic, phenols, lactones groups) were determined by back potentiometric titration with 0.05 M NaOH solution [28,29]. The sulfonic group content was determined from solution d by direct titration with a NaOH (0.05 M) solution [28]. Measurement of

each sample was conducted in triplicate and the average values were reported.

2.5. *Jatropha* biodiesel production and analysis

Jatropha oil was esterified with solid acid, and subsequently transesterified to biodiesel with solid base. The synthesized biodiesel was analyzed by gas chromatography (GC).

2.5.1. Pretreatment (esterification) of crude *Jatropha* oil

Crude oil (27.9 g or 0.03 mol) was mixed with the magnetic C-SO₃H@Fe/JHC acid (2.5–12.5 wt%) in a 50-mL reactor lined with a quartz cup (YZPR-50, Shanghai Yanzheng Experimental Instrument Co., Ltd.). The reactor was filled by N₂ with initial pressure of 1.9–2.1 MPa to avoid methanol evaporation to its dead volume (9.6 mL) during reaction. The esterification was conducted at 60–100 °C for 30–150 min with a stirring speed of 750 rpm. After reaction, catalyst was isolated by an NdFeB magnet (Scheme 1b) and submitted for cycles without washing. The esterified *Jatropha* oil (EJO) was collected and filtered through a 0.22-μm filter. The AV and saponification value (SV) of oils were measured by titration according to the standard methods of American Society for Testing and Materials [ASTM, D1980-87(1998) and D5558-95(2011)], respectively. The molecular weight (*M*) was calculated by the equation of $[M = (56.1 \times 1000 \times 3)/(SV-AV)]$ [30].

After 3 or 5 reaction cycles for C-SO₃H@Fe/JHC, the catalysts (designated as C-SO₃H@Fe/JHC-3 or C-SO₃H@Fe/JHC-5) were recovered by a 3-time washing with 20 mL ethanol followed by drying at 85 °C for 2 h with a nitrogen flow rate of 200 mL/min. The washed recovered catalysts were recycled further, similarly, C-SO₃H@Fe/JHC-R6 and C-SO₃H@Fe/JHC-R9 were recovered catalysts after 6 and 9 cycles for esterification, respectively. The recovery yield of catalyst was defined as:

$$\text{Catalyst recovery (\%)} = \frac{\text{mass of recovered catalyst (g)}}{\text{mass of catalyst submitted to the reaction (g)}} \times 100\% \quad (1)$$

2.5.2. Production of *Jatropha* biodiesel

EJO (0.3 mol) and related dehydrated methanol were loaded in the YZPR-50 reactor containing certain amount of the magnetic base Na₂SiO₃@Ni/JRC for transesterification at 55–75 °C for 60–140 min with a stirring speed of 750 rpm. After reaction, the magnetic base catalyst was separated for cycles (Scheme 1c) without washing. The upper-layer (biodiesel product) was analyzed using GC (GC-2014, Shimadzu, Kyoto) equipped with a capillary column (Rtx-Wax, 30 m × 0.25 mm × 0.25 μm, Restek Corporation, Bellefonte, PA) and a flame ionization detector (FID, 221-70162-9, Shimadzu). The crude biodiesel was diluted with CH₂Cl₂. The injection volume was 1.0 μL with a split ratio 40/1. Temperatures of column, injector and detector were set at 220 °C, 260 °C and 280 °C, respectively. Helium (1 mL/min, 99.999% purity) was used as the carrier gas. To quantify the FAMES composition, C_{17:0} was used as an internal standard with calibrated relative response factors of 1.014, 1.023, 1.076, 1.038, 1.019 and 0.926 for the methyl esters of C_{16:0}, C_{16:1}, C_{18:0}, C_{18:1}, C_{18:2} and C_{18:3}, respectively [31]. Biodiesel yield was defined as the weight percentage of all the FAMES in the crude biodiesel [31].

After 3 or 5 reaction cycles for Na₂SiO₃@Ni/JRC, the catalysts (similarly designated as Na₂SiO₃@Ni/JRC-3 or Na₂SiO₃@Ni/JRC-5) were recovered and washed by the method described above. The washed recovered base catalysts were recycled further, similarly, Na₂SiO₃@Ni/JRC-R6 and Na₂SiO₃@Ni/JRC-R9 were recovered base catalysts after 6 and 9 cycles for transesterification, respectively.

2.6. Hydrothermal gasification of glycerol and analysis

A 15 g water, 0.43–0.48 g glycerol and the appropriate amount of the ethanol-washed deactivated base catalyst were loaded in a 25-mL Hastelloy autoclave (HC-276, Parr Instrument Co., Moline, IL) with an 8.4 mL headspace. Before reaction, the autoclave was sealed and filled with 8.0 MPa N₂ (99.999% purity). The autoclave was gradually heated up to 350 °C in a 54–56 min period with a stirring speed of 250 rpm. When reached 350 °C, temperature was retained for 24–26 min under pressure of 21.5–22.0 MPa.

The gas produced was collected in a gasbag after the autoclave was cooling down to low temperatures (25–35 °C) in 2–2.5 h (Scheme 1d). A wet gas meter (LMF-1, Shanghai A.K. Instruments Co., Ltd.) was used for determination of the gas volume. The aqueous phase was centrifuged and submitted to TOC and inorganic carbon (IC) analyses using a TOC analyzer (TOC-VCP_N, Shimadzu). C₆H₄(COOK)(COOH) and Na₂CO₃ were used as calibrating standards. Gas compositions were analyzed by GC (7820A, Agilent, Palo Alto, CA) equipped with a thermal conductivity detector (TCD), and a packed Porapak N column (3 ft × 1/8 in. for H₂, CO₂, C₂H₆, C₂H₄ and C₂H₂) and molecular sieve 5A (6 ft × 1/8 in. for CH₄ and CO). The conditions for analysis were followed by Ref. [21].

The glucose, xylose, 5-hydroxymethylfurfural (HMF), furfural, glycerol, methanol and formaldehyde in the *Jatropha*-hull hydrolysate or liquid products after gasification were determined by a high performance liquid chromatography (HPLC; LC-20A, Shimadzu). Gasification yield and glycerol conversion yield were calculated as below:

$$\begin{aligned} \text{Gasification yield (mol\%)} \\ &= \frac{\text{(mole of inorganic carbon in the aqueous, CO}_2\text{, CH}_4\text{ and CO)}}{\text{(mole of carbon in glycerol)}} \times 100\% \quad (2) \end{aligned}$$

$$\begin{aligned} \text{Conversion yield (wt\%)} \\ &= \left[1 - \frac{\text{(mass of residual glycerol after reaction, mg)}}{\text{(mass of glycerol before reaction, mg)}} \right] \times 100\% \quad (3) \end{aligned}$$

3. Results and discussion

3.1. Catalyst characterization

3.1.1. SEM and BET

The magnetic supporter (C@Fe/JHC) showed a morphology of agglomerated rough particles (<30 μm) with tiny porous on the particle surface (Fig. 1A-a). It had a reduced size (about 2 vs. 10 μm) against the AC-600@Fe/C supporter prepared using glucose as the carbon resource and pyrolyzed at 600 °C [14]. After the sulfonation process, specific surface area and pore volume of the magnetic C-SO₃H@Fe/JHC acid increased from 53.7 and 0.091 to 99.6 m²/g and 0.121 cm³/g, respectively (Fig. S1A-a vs. b). The increases may be caused by the formation of numerous spherical nanoparticles that appeared on the catalyst surface (Fig. 1A-b), as well as the corrosion of C@Fe/JHC and Fe₃C by H₂SO₄ solution during sulfonation (Fig. S2A-a vs. b) [32]. C-SO₃H@Fe/JHC acid achieved a higher biodiesel yield (93.6% vs. 90.5%) than AC-600-SO₃H@Fe/C catalyst (sulfureted from AC-600@Fe/C) with a larger particle size (about 10 μm). It was inferred that catalyst size could affect catalytic activity. Catalyst with smaller size usually possesses large specific area which promises increased contact opportunity with the substrates [21].

Compared to bamboo powders that were used as catalyst supporter [21], the residue collected in the *Jatropha*-hull hydrolysis showed a higher specific surface (15.6 vs. 0.14 m²/g) and larger pore volume (0.072 vs. 0.005 cm³/g). It was possibly caused by the leaching of acid-soluble contents from the solid structure of

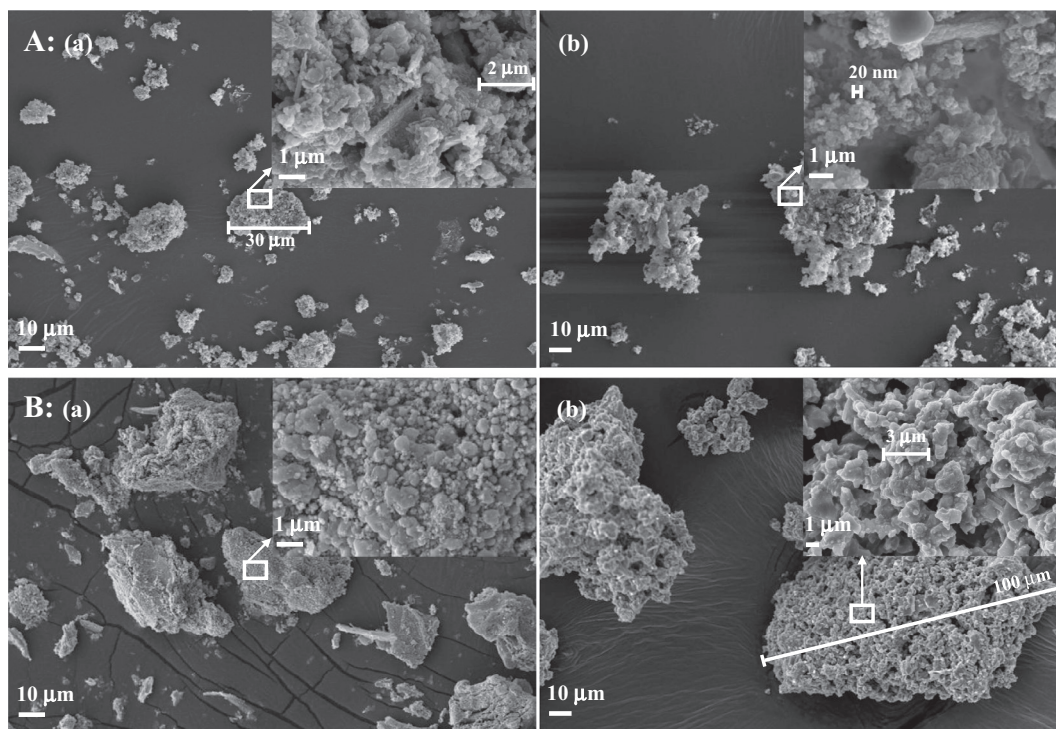


Fig. 1. SEM images of the carbonaceous supporters and catalysts. A: (a) C@Fe/JHC, (b) C-SO₃H@Fe/JHC; B: (a) Ni/JRC, (b) Na₂SiO₃@Ni/JRC.

Jatropha-hull powders. Ni/JRC as base support showed a similar fibrous shape with numerous spherical Ni particles (<1.5 μm) well deposited on the surface (Fig. 1B-a). The size of Na₂SiO₃@Ni/JRC base was <100 μm but with small particles (about 3 μm) agglomerated on the catalyst surface with Na₂SiO₃ gel (Fig. 1B-b). After loading of Na₂SiO₃ gel on Ni/JRC, the specific surface area and pore volume of Na₂SiO₃@Ni/JRC declined from 76.1 to 12.2 m²/g, and from 0.101 to 0.018 cm³/g, respectively (Fig. S1B-a vs. b) [21].

3.1.2. XRD, VSM and ICP-OES

The crystalline phases of Fe, Fe₃C, Fe₂O₃, Ni, Na₂SiO₃ as well as the aromatic carbon sheets [14,33] on the magnetic supporters or catalysts were identified separately according to the Powder Diffraction Standards (06-0696, 72-1110, 39-1346, 04-0850 and 16-0818) and Refs. [14,33], respectively. It was revealed that the formation of Fe and Fe₃C crystalline structures in C@Fe/JHC supporter through reactions of [Fe₃O₄ + C → Fe + CO₂/CO↑, Fe + C → Fe₃C] [14] by the symmetric XRD reflections (Fig. S2A-a). The average size of the crystal Fe was about 106 nm calculated with the Scherrer equation [34]. After sulfonation, the XRD pattern of C-SO₃H@Fe/JHC was dramatically changed for the reduction of Fe size to 42.5 nm from 106 nm as well as with an appearance of Fe₂O₃ phase (Fig. S2A-b) [14]. However, the formation of Fe₂O₃ [Fe + H₂SO₄ → Fe₂O₃ + H₂O + SO₂↑] on the surface could protect the Fe component from further corrosion in concentrated H₂SO₄ [14]. The formation of an amorphous aromatic carbon sheet structure with random orientations could be confirmed in C-SO₃H@Fe/JHC by a strong but broad diffraction peak signal at 2-theta of 20–30° [33,35]. Both magnetic Ni/JRC and Na₂SiO₃@Ni/JRC contained Ni structure. Moreover, there was an additional Na₂SiO₃ symmetric reflection in the XRD pattern of Na₂SiO₃@Ni/JRC, indicating a successful loading of Na₂SiO₃ component on Ni/JRC supporter.

The existence of Fe and Fe₃C (Fig. S2A-a) promoted the magnetic saturation (Ms) of C@Fe/JHC supporter to 83.9 Am²/kg (Fig. S3A-a) [36]. However, Ms of C-SO₃H@Fe/JHC declined to

11.2 Am²/kg (Fig. S3A-b). It could be attributed by the dissolution of Fe and Fe₃C compositions during sulfonation [14]. The Na₂SiO₃ coating on Ni/JRC particles reduced Ms of Na₂SiO₃@Ni/JRC from 59.9 to 15.0 Am²/kg (Fig. S3B a and b). The synthesized Na₂SiO₃@Ni/JRC base in this study had a higher magnetism than the reported Na₂SiO₃/Fe₃O₄ catalyst with Ms of only 0.5 Am²/kg [20]. The higher Ms would benefit an improved efficiency on magnetic separation of Na₂SiO₃@Ni/JRC from biodiesel products (Scheme 1c).

ICP-OES analysis showed a composition (w/w) of 91.6% Ni and 8.40% char with trace elements of 0.03% Na and 0.07% Si in Ni/JRC (Table S1). In Na₂SiO₃@Ni/JRC, Ni content dropped from 91.6 to 25.6 wt% with increased Na, Si and O contents to 27.7, 16.5 and 28.2–28.9 wt%, respectively [21]. After 3 cycles, Ni content increased to 30.2 wt% while Na and Si contents declined to 18.4 and 11.3 wt%, respectively. It could be explained by the release of Na₂SiO₃ from the catalyst in the reaction media [6,21]. In the crude glycerol, the determined contents of Na and Si were 3.12 and 1.67 wt% with trace 0.130 wt% Ni.

3.1.3. FT-IR, TPD and acid-group titration

Both C@Fe/JHC and C-SO₃H@Fe/JHC catalysts showed similar infrared absorptions at 3460 and 1610 cm⁻¹ (Fig. S4A) that demonstrate the O–H and C=O stretching vibrations in phenolic –OH or –COOH groups [18], respectively. Absorbances of C–O–S and O=S=O stretching vibrations at 1060 and 1180 cm⁻¹ indicated the existence of –SO₃H groups in C-SO₃H@Fe/JHC (Fig. S4A-b). Through NH₃-TPD analysis, the total acid content of C@Fe/JHC was only 0.83 mmol/g but it was promoted to 2.96 mmol/g after sulfonation (Fig. 2A). The value was lower than the total acid content determined by the titration method, which was 3.78 mmol/g (Table S2).

Compared to the reported AC-600-SO₃H@Fe/C acid derived from glucose [14], C-SO₃H@Fe/JHC acid showed a larger specific surface area (99.6 vs. 88.9 m²/g), attributed to the existence of smaller particles (about 20 nm vs. 5 μm) on the catalyst surface.

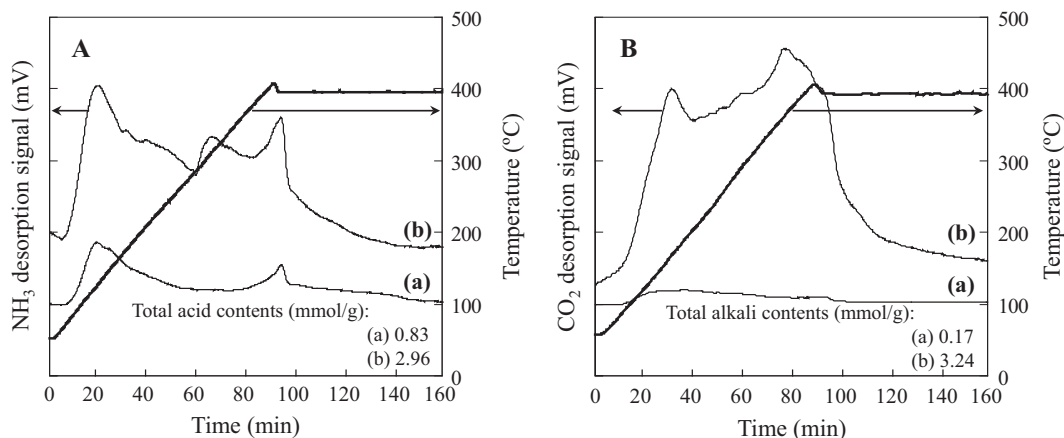


Fig. 2. TPD curves of the carbonaceous supporters and catalysts. A: (a) C@Fe/JHC, (b) C-SO₃H@Fe/JHC; B: (a) Ni/JRC, (b) Na₂SiO₃@Ni/JRC.

On the other hand, C-SO₃H@Fe/JHC acid possessed higher contents of carboxylic and sulfonic groups (1.13 and 1.65 mmol/g vs. 0.92 and 1.27 mmol/g) than that of AC-600-SO₃H@Fe/C. The differences of acid-group density between the two carbon solid acids may not only rely on their distinct specific surface areas but also their origins from different carbon resources [37]. Li et al. [38] showed that furfural produced from xylose or *Jatropha* hulls [39] could be subsequently converted to γ -butyrolactone with a high conversion yield in hydrolysates. The soluble carbon sources such as 26.7 g/L xylose, 11.8 g/L HMF and 7.90 g/L furfural that were found in the *Jatropha*-hull hydrolysate might have played key roles in generating additional lactonic groups on C@Fe/JHC supporter. A higher content of lactonic groups (1.41 vs. 0.59 mmol/g) could lead to the formation of extra phenols, carboxylic and sulfonic groups on C@Fe/JHC through the reactions (Fig. S5) [28], which could have contributed to the promoted content of acid groups on the C-SO₃H@Fe/JHC catalyst.

Other than the -OH group, there was no significant FT-IR absorbance of functional groups in Ni/JRC (Fig. S4B-a), indicating a complete reduction of NiO in Ni/JRC [40,41]. After loading of Na₂SiO₃, Na₂SiO₃@Ni/JRC catalyst showed several FT-IR absorbance peaks from wave-numbers of 710 to 1025 cm⁻¹ (Fig. S4 B-b), such as Si-O bending, Si-O-Na, Si-O-H and Si-O-Si stretching vibrations [42]. In addition, the absorbances at 745 and 467 cm⁻¹ were attributed to the symmetric stretching and bending vibrations of Si-O-Si bond [43]. The absorbance at 1462 cm⁻¹ was for the CO₃²⁻ group, which could be formed by absorption of CO₂ in the air through reactions of [Na₂SiO₃ + CO₂ + H₂O → Na₂CO₃ + H₂SiO₃] [44]. This phenomenon revealed a high sensitivity of Na₂SiO₃@Ni/JRC to CO₂. TPD analysis showed that loading of Na₂SiO₃ significantly promoted the total alkali content of Ni/JRC from 0.17 to 3.24 mmol/g of Na₂SiO₃@Ni/JRC (Fig. 2B). It was also observed an agglomeration of the Na₂SiO₃ gel (~3 μ m in size) on Na₂SiO₃@Ni/JRC (Fig. 1B-b). The solid base catalyst synthesized in this study showed a higher total alkali content against the Na₂SiO₃@Ni/C derived from bamboo powders (3.24 vs. 3.18 mmol/g) [21]

3.2. Esterification of crude *Jatropha* oil using solid acid

The synthesized C-SO₃H@Fe/JHC was applied in the esterification of crude *Jatropha* oil with a high AV of 17.2 mg KOH/g. Effects of catalyst dosage (2.5–12.5 wt% of oil), reaction temperature (60–100 °C), reaction time (30–150 min) and molar ratio of methanol/oil (6/1–18/1) on the AV reduction were investigated using a single factor test design (Fig. S6).

3.2.1. Catalyst dosage

Under the reaction conditions of 80 °C and 90 min with methanol/oil ratio of 12/1, a gradual increase of catalyst from 2.5 to 10 wt % led to a remarkable decline of AV from 15.4 to 6.05 mg KOH/g (Fig. S5a). However, a further increase in catalyst to 12.5 wt% had AV slightly increased to 6.15 mg KOH/g. The disproportionate correlation between catalyst dosage and AV indicated a great challenge in fully mixing liquid reactants with heterogeneous catalyst in the magnetically stirred reactor [14,21]. Therefore, 10 wt% catalyst was selected to be used in the following experiments.

3.2.2. Reaction temperature

Under the conditions of 90 min and 10 wt% catalyst with 12/1 methanol/oil ratio, AV decreased sharply from 16.9 to 2.05 mg KOH/g with an increase of temperature from 60 to 90 °C (Fig. S6b). As higher temperature (100 °C) only contributed a slight reduction in AV to 1.95 mg KOH/g, 90 °C was selected as reaction temperature in the following experiments [15].

3.2.3. Reaction time

Reacted at 12/1 methanol/oil molar ratio and 90 °C, AV decreased from 10.5 to 1.3 mg KOH/g when time was prolonged from 30 to 120 min. The further extension of time to 150 min only achieved an AV of 1.1 mg KOH/g (Fig. S6c) [15]. Since there was little change of AV from 120 to 150 min, 120 min was used as the reaction time in the following experiments.

3.2.4. Methanol/oil molar ratio

As methanol possesses a boiling point (64.7 °C) below most of the reaction temperatures applied in this study, excessive methanol was usually supplied (with methanol/oil ratio from 6/1 to 18/1) to compensate the methanol evaporated to the dead volume of the reactor (Fig. S6d). When methanol/oil molar ratio increased from 6/1 to 12/1, AV remarkably decreased from 11.5 to 1.30 mg KOH/g. However, a further increase in methanol/oil molar ratio from 15/1 to 18/1 could have the relative consistency of catalyst intensively diluted in the reacting mixture and led to a slight increase of AV from 1.5 to 1.8 mg KOH/g, respectively [14]. The value of 12/1 methanol/oil molar ratio was selected.

Under the reaction conditions of 90 °C, 120 min, 10 wt% catalyst and 12/1 methanol/oil molar ratio, crude *Jatropha* oil could be efficiently esterified using C-SO₃H@Fe/JHC acid. The AV of the oil decreased from 17.2 to 1.3 mg KOH/g, with a reduction by 92.44%. The low AV oil was used for the base transesterification to produce biodiesel.

3.3. Biodiesel production with solid base

The esterified oil with an AV of 1.3 mg KOH/g was reacted with methanol catalyzed with base $\text{Na}_2\text{SiO}_3@Ni/JRC$. Effects of methanol/oil molar ratio (3/1–15/1), catalyst dosage (3–11, wt%), reaction temperature (55–75 °C), and reaction time (60–140 min) on biodiesel yield were investigated using a single-factor test design (Fig. S7).

3.3.1. Methanol/oil molar ratio

When applying 5 wt% catalyst at 65 °C for 100 min with theoretical methanol/oil ratio of 3/1, methanol evaporation caused insufficient alcohol for the transesterification reaction [31], only

56.7% biodiesel yield was produced. As methanol/oil molar ratio increased from 6/1 to 9/1, biodiesel yield was promoted to 83.3% and further reached the peak value of 91.3% (Fig. S7a). However, an intensive increase of methanol had a negative effect on biodiesel yield. With methanol/oil molar ratio increased from 12/1 to 15/1, biodiesel yield dropped from 89.2% to 88.1%, respectively [31]. Methanol/oil molar ratio was selected as 9/1.

3.3.2. Catalyst dosage

In Fig. S7b, when catalyst increased from 3 to 7 wt%, biodiesel yield reached the highest value of 94.7%. However, further increase of catalyst from 9 to 11 wt% led to a slight decline of biodiesel yield from 93.2% to 92.3%. It could be explained by an insufficient distri-

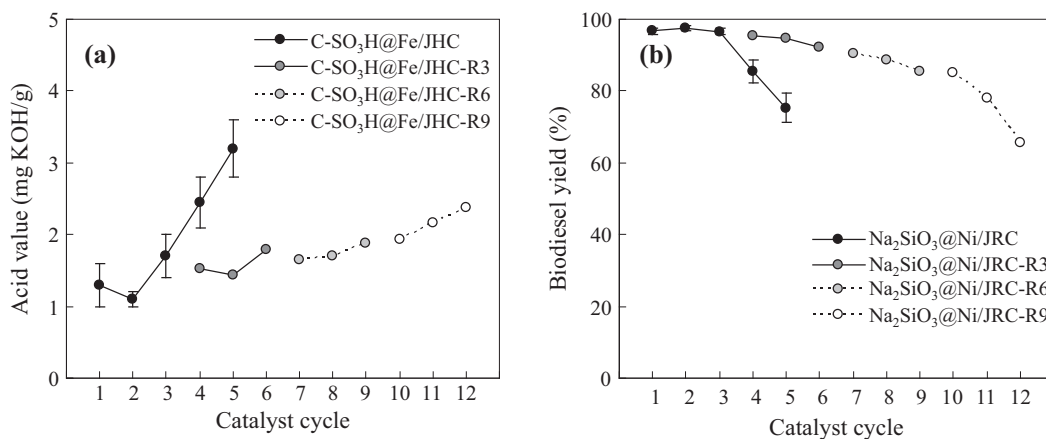


Fig. 3. Cycle of catalysts for (a) crude *Jatropha* oil esterified with C-SO₃H@Fe/JHC acid and (b) biodiesel production with Na₂SiO₃@Ni/JRC base. [Reaction conditions: (a) 10 wt% catalyst loading with 12/1 methanol/oil molar ratio, at 90 °C for 120 min; and (b) 7 wt% catalyst loading with 9/1 methanol/oil molar ratio, at 65 °C for 120 min.]

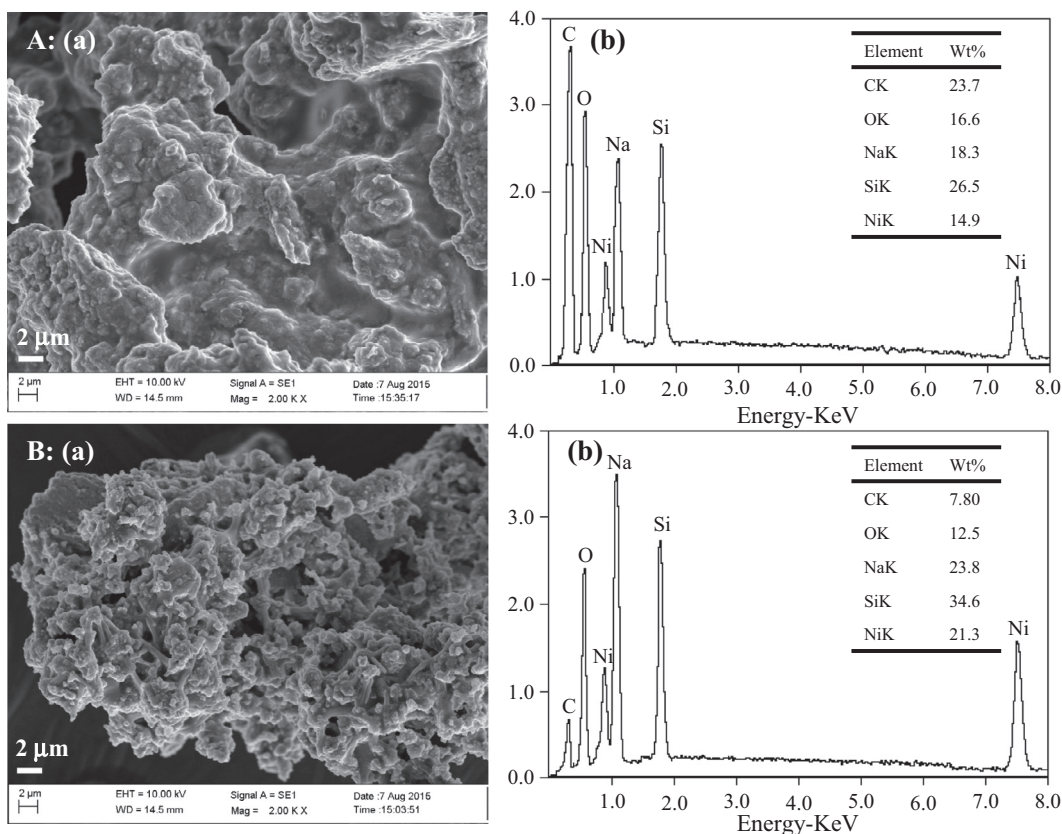


Fig. 4. (a) SEM images and (b) EDX graphics of (A) unwashed magnetic Na₂SiO₃@Ni/JRC-3 catalyst and (B) washed magnetic Na₂SiO₃@Ni/JRC-R3 catalyst.

bution of catalyst in the reaction system with the magnetic stirring method [21]. Catalyst dosage was selected as 7 wt%.

3.3.3. Reaction temperature

With reaction time of 100 min, biodiesel yield was only 78.0% at 55 °C. An increase in temperature to 65 °C achieved the highest biodiesel yield of 94.7% (Fig. S7c). A higher temperature at 75 °C had the biodiesel yield declined to 87.2%. Although high temperature promoted chemical reaction rate, evaporation of methanol that could result in lowering biodiesel yield should also be considered [45]. For balancing a high reaction rate with less methanol evaporation, 65 °C was recognized as the relative optimal temperature for biodiesel production in this study.

3.3.4. Reaction time

Biodiesel yield continuously increased from 87.4% to 96.7% with reaction time increased from 60 to 120 min (Fig. S7d). As the transesterification is a reversible conversion reaction [21], biodiesel yield slightly decreased to 95.6% with a prolonged reaction time to 140 min. Reaction time was selected as 120 min.

In total, the relative optimal conditions for biodiesel production with $\text{Na}_2\text{SiO}_3@Ni/JRC$ base were: 7 wt% catalyst at 65 °C for 120 min with 9/1 methanol/oil molar ratio. Under these conditions, biodiesel yield reached 96.7%.

3.4. Catalyst cycles

Under the optimal conditions obtained above, the recycle of both $\text{C-SO}_3\text{H@Fe/JHC}$ for esterification and $\text{Na}_2\text{SiO}_3@Ni/JRC$ for transesterification was performed, respectively (Fig. 3).

Both solid acid and base catalysts showed a decline in catalyzing efficiencies after several cycles. With an average recovery yield of 90.3 ± 3.17 wt%, a 5-cycle use of $\text{C-SO}_3\text{H@Fe/JHC}$ acid in esterifying the crude *Jatropha* oil led to the AV reduced to 1.30, 1.10, 1.70, 2.45 and 3.20 mg KOH/g, respectively (Fig. 3a). $\text{Na}_2\text{SiO}_3@Ni/JRC$ base was also recycled in the transesterification of EJO for biodiesel production. There were no significant differences in biodiesel yields among the 1st, 2nd and 3rd cycle of the solid base, with 96.7%, 97.5% and 96.5% yields, respectively (Fig. 3b) [10]. However, biodiesel yield dropped to 85.6% and 75.3% in the 4th and 5th cycle, respectively [21]. The average recovery yield of the solid base was 86.7 ± 2.56 wt% for the 5 cycles.

For $\text{C-SO}_3\text{H@Fe/JHC-3}$, the calculated content of sulfonic group ($-\text{SO}_3\text{H}$) was 0.506 mmol/g assuming that all S atoms were only associated in the $-\text{SO}_3\text{H}$ group. Compared to the original $\text{C-SO}_3\text{H@Fe/JHC}$ acid, the content (wt%) of S in the unwashed $\text{C-SO}_3\text{H@Fe/JHC-3}$ showed a remarkable decrease from 3.56 to 1.62 wt% (Table S3). At the meantime, the C and H contents (wt%) increased from 38.6 to 45.9, and 2.10 to 5.37, respectively. The N and Fe contents (wt%) decreased from 1.14 to 0.71, and 26.7 to 17.4, respectively. After washed, the recovered $\text{C-SO}_3\text{H@Fe/JHC-3}$ acid had similar elemental compositions of C, H, N, S and Fe to that for the original $\text{C-SO}_3\text{H@Fe/JHC}$ catalyst (wt%, 39.6, 2.63, 1.08, 3.39 and 25.6 vs. 38.6, 2.10, 1.14, 3.56 and 26.7) because organics were removed that have high content of C and H.

As for the solid base, compared to the original $\text{Na}_2\text{SiO}_3@Ni/JRC$ (Fig. 1B-b), a dramatic change in morphology was observed for the unwashed $\text{Na}_2\text{SiO}_3@Ni/JRC-3$ base (Fig. 4A-a) possibly due to being covered by oil and formed soap (Fig. 4A-a). But, the washed $\text{Na}_2\text{SiO}_3@Ni/JRC-R3$ base (Fig. 4B-a) had some cracks or minor fragments on the surface, similar to that of the original $\text{Na}_2\text{SiO}_3@Ni/JRC$ base (vs. Fig. 1B-b). EDX analysis showed an elementary composition (wt%) of C (23.7), O (16.6), Na (18.3), Si (26.5) and Ni (14.9) on the unwashed $\text{Na}_2\text{SiO}_3@Ni/JRC-3$ surface (Fig. 4A-b). Compared to the washed $\text{Na}_2\text{SiO}_3@Ni/JRC-R3$, the higher contents of C and O on the unwashed $\text{Na}_2\text{SiO}_3@Ni/JRC-3$ (23.7 and 16.6 vs. 7.80 and 12.5) could be caused by the existence of glycerol, biodiesel or oil residuals deposited within the interior structure of the catalyst. The washed recovered $\text{C-SO}_3\text{H@Fe/JHC-R3}$ acid and $\text{Na}_2\text{SiO}_3@Ni/JRC-R3$ base were cycled in the esterification and transesterification, respectively. Results showed that the average AV of EJO was ≤ 1.80 mg KOH/g (1.53, 1.44 and 1.80) with $\text{C-SO}_3\text{H@Fe/JHC-R3}$ and biodiesel yield was $>92.0\%$ (95.5, 94.8 and 92.4) with $\text{Na}_2\text{SiO}_3@Ni/JRC-R3$ in 3 cycles (Fig. 3).

Both $\text{C-SO}_3\text{H@Fe/JHC}$ and $\text{Na}_2\text{SiO}_3@Ni/JRC$ catalysts possessed a good reusability. It was revealed that the binding of active sites by the crude glycerol or other residuals from the oil was the main cause of the catalyst deactivation [21]. An ethanol-wash could simply realize the recovery of catalyst activities. With an intensive recycle of the recovered catalysts for 10 cycles, AV of the EJO was still below 2.0 mg KOH/g with biodiesel yield remained above 85% (Fig. 3).

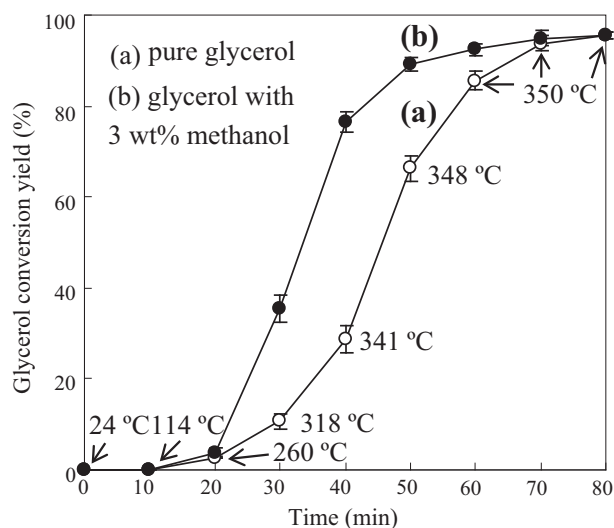


Fig. 5. Glycerol conversion yield through hydrothermal gasification with the washed deactivated $\text{Na}_2\text{SiO}_3@Ni/JRC-R3$ (a) pure glycerol (b) pure glycerol blended with 3 wt% methanol. [Reaction conditions: 0.46 g pure glycerol and 15 g H_2O sealed in the autoclave with 8.0 MPa N_2 , the autoclave was heated for 55 min to reach 350 °C. The reaction was maintained at 350 °C for 25 min with a highest pressure of 22.0 MPa.]

Table 1

Gasification yields (mmol) and gas compositions (mol%) in the hydrothermal gasification of glycerol with Ni/JRC or the washed $\text{Na}_2\text{SiO}_3@Ni/JRC-R3$.

Gas products	Ni/JRC ^a	$\text{Na}_2\text{SiO}_3@Ni/JRC-R3^a$	Ni/JRC ^b	$\text{Na}_2\text{SiO}_3@Ni/JRC-R3^b$
H_2	8.07, 58.8 ± 0.89	12.5, 73.5 ± 2.09	9.82, 67.4 ± 2.51	13.2, 81.7 ± 3.29
CO	0.00777, 0.06 ± 0.01	0.0154, 0.09 ± 0.01	0.0129, 0.09 ± 0.01	0.0208, 0.13 ± 0.01
CH_4	0.851, 6.20 ± 0.70	1.17, 6.91 ± 0.23	1.02, 7.00 ± 0.78	0.978, 6.05 ± 0.90
CO_2	4.79, 34.9 ± 2.96	3.30, 19.5 ± 1.99	3.71, 25.5 ± 2.77	1.97, 12.1 ± 0.82
$\text{C}_2\text{H}_2, \text{C}_2\text{H}_4, \text{C}_2\text{H}_6$	<0.01	<0.01	<0.01	<0.01

Reaction conditions: 0.46 g glycerol (total carbon 15 mmol), 15 g H_2O and 33 wt% Ni/JRC or 100 wt% $\text{Na}_2\text{SiO}_3@Ni/JRC-R3$ in the autoclave with 8.0 MPa N_2 . Reaction was conducted at 350 °C for 4–6 min at 22.0 MPa. Using ^a pure glycerol or ^b crude glycerol as the reaction substrate.

Table 2
Carbon balance and glycerol gasification yields with Ni/JRC or the washed Na₂SiO₃@Ni/JRC-R3.

Components (mol%)	Ni/JRC ^a	Na ₂ SiO ₃ @Ni/JRC-R3 ^a	Ni/JRC ^b	Na ₂ SiO ₃ @Ni/JRC-R3 ^b
Carbon in aqueous-phase	56.7	73.3	66.1	78.9
Inorganic carbon	4.30 ± 0.15	46.1 ± 1.26	20.3 ± 0.78	62.7 ± 2.13
Organic carbon	52.4 ± 1.73	27.2 ± 0.84	45.8 ± 1.21	16.2 ± 0.76
Carbon in gas-phase	41.2	26.5	32.6	18.3
Total carbon	97.9	99.8	98.7	97.2
Glycerol gasification yield	45.5	72.6	52.9	81.0

Reaction condition was the same as Table 1.

Using ^a pure glycerol or ^b crude glycerol as the reaction substrate.

3.5. Hydrothermal gasification of the glycerol by-product

The Ni/JRC supporter and washed deactivated Na₂SiO₃@Ni/JRC-R3 base were used for the hydrothermal gasification of glycerol for H₂ production. The reaction was conducted at 350 °C for 24–26 min (Fig. S8). Without adding any catalyst, gasification yield was extremely low with 0.102 H₂, 0.00352 CO, 0.0702 CH₄, and 0.468 CO₂ (mmol) produced from pure glycerol with a total carbon loading of 15 mmol. When using Ni/JRC, the H₂, CO, CH₄ and CO₂ yields were promoted remarkably to 8.07, 0.00777, 0.851 and 4.79 (mmol), respectively (Table 1). It could be explained by the high activity of Ni/JRC in catalyzing the water-gas shift reaction (C₃H₈O₃ + H₂O → CO₂/CO + H₂) and the methanation reaction (CO + H₂ → CH₄ + H₂O) [46,47].

With the deactivated Na₂SiO₃@Ni/JRC-R3 base (containing 30.2 wt% Ni, Table S1), H₂-rich gas (13.2 H₂, 0.0208 CO, 0.978 CH₄ and 1.97 CO₂, mmol, Table 1) was produced from the crude glycerol. Compared to the deactivated Na₂SiO₃@Ni/C catalyst derived from bamboo in previous work [21], the deactivated Na₂SiO₃@Ni/JRC-R3 base had more Na₂SiO₃ remained on the catalyst (18.4 and 11.3 Na and Si wt% vs. 8.21 and 5.09, Table S1). It provided a higher activity in catalyzing glycerol gasification in the absence of additional Na₂CO₃. It was found that using the crude glycerol could achieve a higher gas yield as well as a higher glycerol conversion yield than the pure glycerol (Table 1).

The conversion yield of pure glycerol was only between 0 to 16.7 wt% when temperature was raised up from 114 to 318 °C with the deactivated Na₂SiO₃@Ni/JRC-R3 base (Fig. 5a). As temperature increased to 350 °C, a sharp increase in conversion yield (85.6 wt %) was achieved with gasification yield of 72.6 mol% (Table 2) and H₂ purification of 73.5 mol% (Table 1). As time extended to 10 and 20 min, conversion yield reached 93.7% and 95.5%, respectively. Similarly, Samad et al. [49] reported that glycerol degradation and methanol production was enhanced by increasing temperature up to 300 °C. The dramatic promotion on conversion yield could be attributed to high temperature, as well as the high concentration of OH⁻ and H⁺ from water as the decrease in the dielectric constant at temperature close to the critical point of water (>374 °C and 22.1 MPa) [46,48]. Methanol also played a role for the rise.

It was found that using the crude glycerol produced from the catalytic transesterification achieved a higher gas yield with a higher glycerol conversion yield than using pure glycerol (Table 1). On one hand, it was indicated that the leached Na⁺ and Si⁴⁺ ions (3.12 wt% Na and 1.67 wt% Si, Table S1) in the crude glycerol had played a positive role in promoting the hydrothermal gasification reaction (Table 2) [21]. When using Na₂SiO₃@Ni/JRC for the transesterification, the leached free Na₂SiO₃ could form Na₂CO₃ in the crude glycerol by reacting with CO₂ from the air through reaction of [CO₂ + H₂O + Na₂SiO₃ → Na₂CO₃ + H₂SiO₃]. The IC analysis showed a higher dissolved inorganic carbon content in the gasification of the crude glycerol than pure glycerol (20.3 vs. 4.30 mol%) with Ni/JRC (Table 2). The Na₂CO₃ in the crude glycerol could be

of help in promoting gasification yield from 45.5 to 52.9 mol% with Ni/JRC or from 72.6 to 81.0 mol% with the deactivated Na₂SiO₃@Ni/JRC-R3, respectively (Table 2) [48]. Moreover, the adsorption of CO₂ could lead to a higher H₂ composition using the crude glycerol (Table 1). On the other hand, the crude glycerol (with carbon content of 32.7 mmol/g) produced during *Jatropha* biodiesel production contained 93.6 wt% glycerol and 2.72 wt% methanol. In order to confirm the positive effect of residual methanol composition on promoting glycerol conversion, pure glycerol blended with 3.0 wt% methanol was submitted to the hydrothermal gasification with the deactivated Na₂SiO₃@Ni/JRC-R3 (Fig. 5b). The glycerol conversion yield increased remarkably from 3.7 to 76.6 wt% when temperature rose from 260 to 341 °C within 20 min. The methanol in the crude glycerol (Table 2) may have acted as a promoter for glycerol conversion. With an increase in temperature from 220 to 320 °C, H₂ from the decomposition of methanol through dehydrogenation and gasification (CH₃OH → HCHO + H₂↑, HCHO + H₂O → CO₂↑ + 2H₂↑) [49–51] could trigger the hydrogenation of glycerol to methanol (C₃H₈O₃ + H₂ → CH₃OH) [47], which occurred at a lower temperature. After 60 min, 92.5 wt% conversion yield and 81.0 mol% gasification yield with H₂ purity of 81.7 mol% could be achieved. However, the conversion yield for the glycerol blended with methanol was still less than that for the crude glycerol, which was 93.4 wt%, which confirmed the importance of the Na⁺ and Si⁴⁺ ions leached from Na₂SiO₃@Ni/JRC-R3 into the crude glycerol to facilitate the gasification.

4. Conclusions

Solid C-SO₃H@Fe/JHC acid and Na₂SiO₃@Ni/JRC base, with strong magnetism (Ms of 11.2 and 15.0 Am²/kg) and high content of acid/base sites (2.96 and 3.24 mmol/g) were prepared from *Jatropha* hulls and applied in a two-step biodiesel production by catalyzing the esterification and subsequent transesterification of *Jatropha* oil, respectively. Compared to traditional carbon resources such as glucose and bamboo powders, *Jatropha*-hull hydrolysate or hydrolyzed residue led to a promising carbonaceous supporting structure with abundant functional groups, or high specific surface area and pore volume. The catalysts showed advantages of less corrosion, high recovery as well as stability for at least 10 cycles. Through the hydrothermal gasification with the deactivated Na₂SiO₃@Ni/JRC base, H₂ was produced from the crude glycerol by-product. The research demonstrated a comprehensive green approach to fully utilize the *Jatropha* seeds for the co-production of biodiesel and H₂.

Acknowledgments

The authors wish to acknowledge the financial support from Nanjing Agricultural University (68Q-0603), Youth Innovation Promotion Association CAS (No. 2017440) and Natural Science Foundation of China (No. 31400518).

Appendix A. Supplementary material

Supplementary data associated with this article can be found, in the online version, at <http://dx.doi.org/10.1016/j.enconman.2017.03.026>.

References

- [1] Yokoyama R, Wakui T, Satake R. Prediction of energy demands using neural network with model identification by global optimization. *Energy Convers Manage* 2009;50:319–27.
- [2] Kaarstad O. Fossil fuels and responses to global warming. *Energy Convers Manage* 1995;36:869–72.
- [3] Costa JF, Almeida MF, Alvim-Ferraz MCM, Dias JM. Biodiesel production using oil from fish canning industry wastes. *Energy Convers Manage* 2013;74:17–23.
- [4] Tian XF, Rehmann L, Xu C, Fang Z. Pre-treatment of eastern white pine (*Pinus Strobes* L.) for enzymatic hydrolysis and ethanol production by organic electrolyte solutions. *ACS Sustain Chem Eng* 2016;4:2822–9.
- [5] Kang K, Azargohar R, Dalai AK, Wang H. Hydrogen production from lignin, cellulose and waste biomass via supercritical water gasification: catalyst activity and process optimization study. *Energy Convers Manage* 2016;117:528–37.
- [6] Kwok Q, Acheson B, Turcotte R, Janès A, Marlair G. Thermal hazards related to the use of potassium and sodium methoxides in the biodiesel industry. *J Hazard Mater* 2013;250–251:484–90.
- [7] Xie W, Zhao L. Heterogeneous CaO-MoO₃-SBA-15 catalysts for biodiesel production from soybean oil. *Energy Convers Manage* 2014;79:34–42.
- [8] Yin X, Duan X, You Q, Dai C, Tan Z, Zhu X. Biodiesel production from soybean oil deodorizer distillate using calcined duck eggshell as catalyst. *Energy Convers Manage* 2016;112:199–207.
- [9] Helwani Z, Aziz N, Bakar MZA, Mukhtar H, Kim J, Othman MR. Conversion of *Jatropha curcas* oil into biodiesel using re-crystallized hydrotalcite. *Energy Convers Manage* 2013;73:128–34.
- [10] Zhang F, Fang Z, Wang YT. Biodiesel production directly from oils with high acid value by magnetic Na₂SiO₃@Fe₃O₄/C catalyst and ultrasound. *Fuel* 2015;150:370–7.
- [11] Soh L, Curry J, Beckman EJ, Zimmerman JB. Effect of system conditions for biodiesel production via transesterification using carbon dioxide-methanol mixtures in the presence of a heterogeneous catalyst. *ACS Sustain Chem Eng* 2014;2:387–95.
- [12] Badday AS, Abdullah AZ, Lee KT. Optimization of biodiesel production process from *Jatropha* oil using supported heteropolyacid catalyst and assisted by ultrasonic energy. *Renew Energy* 2013;50:427–32.
- [13] Liu H, Chen JZ, Chen LM, Xu YS, Guo XH, Fang DY. Carbon nanotube-based solid sulfonic acids as catalysts for production of fatty acid methyl ester via transesterification and esterification. *ACS Sustain Chem Eng* 2016;4:3140–50.
- [14] Zhang F, Fang Z, Wang YT. Biodiesel production direct from high acid value oil with a novel magnetic carbonaceous acid. *Appl Energy* 2015;155:637–47.
- [15] Pua FL, Fang Z, Zakaria S, Chia CH, Guo F. Direct production of biodiesel from high-acid value *Jatropha* oil with solid acid catalyst derived from lignin. *Biotechnol Biofuels* 2011;4:56–64.
- [16] Abdelrahman BF, Akram MA, Marwa HAT. Biodiesel production from *Silybum marianum* L. seed oil with high FFA content using sulfonated carbon catalyst for esterification and base catalyst for transesterification. *Energy Convers Manage* 2016;108:255–65.
- [17] Corro G, Pal U, Tellez N. Biodiesel production from *Jatropha curcas* crude oil using ZnO/SiO₂ photocatalyst for free fatty acids esterification. *Appl Catal B – Environ* 2013;129:39–47.
- [18] Srilatha K, Prabhavathi-Devi BLA, Lingaiah N, Prasad RBN, Sai-Prasad PS. Biodiesel production from used cooking oil by two-step heterogeneous catalyzed process. *Bioresour Technol* 2012;119:306–11.
- [19] Lin L, Cui H, Vittayapadung S, Xiao Z, Wu W, Zhang A, et al. Synthesis of recyclable hollow Fe/C-SO₃H fiber as a catalyst for the production of biodiesel. *Environ Prog Sustain Energy* 2014;33:1432–7.
- [20] Guo PM, Huang FH, Zheng MM, Li WL, Huang QD. Magnetic solid base catalysts for the production of biodiesel. *J Am Oil Chem Soc* 2012;89:925–33.
- [21] Zhang F, Wu XH, Yao M, Fang Z, Wang YT. Production of biodiesel and hydrogen from plant oil catalyzed by magnetic carbon-supported nickel and sodium silicate. *Green Chem* 2016;18:3302–14.
- [22] Ong HC, Silitonga AS, Masjuki HH, Mahlia TMI, Chong WT, Boosroh MH. Production and comparative fuel properties of biodiesel from non-edible oils: *Jatropha curcas*, *Sterculia foetida* and *Ceiba pentandra*. *Energy Convers Manage* 2013;73:245–55.
- [23] Yang CY, Fang Z, Li B, Long YF. Review and prospects of *Jatropha* biodiesel industry in China. *Renew Sust Energy Rev* 2012;16:2178–90.
- [24] Castro González NF. International experiences with the cultivation of *Jatropha curcas* for biodiesel production. *Energy* 2016;112:1245–58.
- [25] State Forestry Administration of China. National Forestry Biomass Energy Development Plan (2011–2020). Lin Gui Fa; 2013 [86], p. 10–11 [in Chinese].
- [26] Sharma DK, Pandey AK, Lata. Use of *Jatropha curcas* hull biomass for bioactive compound production. *Biomass Bioenergy* 2009;33:159–62.
- [27] Gonçalves M, Soler FC, Isoda N, Carvalho WA, Mandelli D, Sepúlveda J. Glycerol conversion into value-added products in presence of a green recyclable catalyst: acid black carbon obtained from coffee ground wastes. *J Taiwan Inst Chem Eng* 2016;60:204–301.
- [28] Tamborini LH, Militello MP, Balach J, Moyano JM, Barbero CA, Acevedo DF. Application of sulfonated nanoporous carbons as acid catalysts for Fischer esterification reactions. *Arab J Chem*. <http://dx.doi.org/10.1016/j.arabic.2015.08.018>.
- [29] Oickle AM, Goertzen SL, Hopper KR, Abdalla YO, Andreas HA. Standardization of the Boehm titration: Part II. Method of agitation, effect of filtering and dilute titrant. *Carbon* 2010;48:3313–22.
- [30] Luo H, Fan W, Li Y, Nan G. Biodiesel production using alkaline ionic liquid and adopted as lubricity additive for low-sulfur diesel fuel. *Bioresour Technol* 2013;140:337–41.
- [31] Xue BJ, Luo J, Zhang F, Fang Z. Biodiesel production from soybean and *Jatropha* oils by magnetic CaFe₂O₄-Ca₂Fe₂O₅-based catalyst. *Energy* 2014;68:584–91.
- [32] Hu L, Tang X, Wu Z, Lin L, Xu J, Xu N, et al. Magnetic lignin-derived carbonaceous catalyst for the dehydration of fructose into 5-hydroxymethylfurfural in dimethylsulfoxide. *Chem Eng J* 2015;263:299–308.
- [33] Nakajima K, Hara M. Environmentally benign production of chemicals and energy using a carbon-based strong solid acid. *J Am Ceram Soc* 2007;90:3725–34.
- [34] Liu XR. Catalyst characterization and evaluation. In: Huang ZT, editor. *Handbook of Industrial Catalyst*. Beijing: Chemical Industry Press; 2004. p. 187–99 [in Chinese].
- [35] Dawodu FA, Ayodele O, Xin J, Zhang S, Yan D. Effective conversion of nonedible oil with high free fatty acid into biodiesel by sulphonated carbon catalyst. *Appl Energy* 2014;114:819–26.
- [36] López de Arroyabe Loyo R, Nikitenko SI, Scheinost AC, Simonoff M. Immobilization of selenite on Fe₃O₄ and Fe/Fe₃C ultrasmall particles. *Environ Sci Technol* 2008;42:2451–6.
- [37] Li S, Gu Z, Bjornson BE, Muthukumarappan A. Biochar based solid acid catalyst hydrolyze biomass. *J Environ Chem Eng* 2013;1:1174–81.
- [38] Li X, Lan X, Wang T. Highly selective catalytic conversion of furfural to γ -butyrolactone. *Green Chem* 2016;18:638–42.
- [39] Su TC, Fang Z, Zhang F, Luo J, Li XK. Hydrolysis of selected tropical plant wastes catalyzed by a magnetic carbonaceous acid with microwave. *Sci Rep* 2015;5:17538–42.
- [40] Varshney D, Dwivedi S. Synthesis, structural, Raman spectroscopic and paramagnetic properties of Sn doped NiO nanoparticles. *Superlattices Microstruct* 2015;86:430–7.
- [41] Rownaghi AA, Huhnke RL. Producing hydrogen-rich gases by steam reforming of syngas tar over CaO/MgO/NiO catalysts. *ACS Sustain Chem Eng* 2013;1:80–6.
- [42] Guo F, Wei NN, Xiu ZL, Fang Z. Transesterification mechanism of soybean oil to biodiesel catalyzed by calcined sodium silicate. *Fuel* 2012;93:468–72.
- [43] Chen Y, Yu G, Li F, Wei J. Structure and photoluminescence of amorphous silicate composites containing ZnO particles synthesized from layered sodium silicate. *J Non-Cryst Solids* 2012;358:1772–7.
- [44] Kouassi SS, Tognonvi MT, Soro J, Rossignol S. Consolidation mechanism of materials obtained from sodium silicate solution and silica-based aggregates. *J Non-Cryst Solids* 2011;357:3013–21.
- [45] Deng X, Fang Z, Liu YH, Yu CL. Production of biodiesel from *Jatropha* oil catalyzed by nanosized solid basic catalyst. *Energy* 2011;36:777–84.
- [46] Fang Z, Minowa T, Fang C, Smith Jr RL, Inomata H, Kozinski JA. Catalytic hydrothermal gasification of cellulose and glucose. *Int J Hydrog Energy* 2008;33:981–90.
- [47] Menor M, Sayas S, Chica A. Natural sepiolite promoted with Ni as new and efficient catalyst for the sustainable production of hydrogen by steam reforming of the biodiesel by-products glycerol. *Fuel* 2017;193:351–8.
- [48] Fang Z, Minowa T, Smith Jr RL, Ogi T, Kozinski JA. Liquefaction and gasification of cellulose with Na₂CO₃ and Ni in subcritical water at 350 °C. *Ind Eng Chem Res* 2004;43:2454–63.
- [49] Samad WZ, Goto M, Kanda H, Wahyudiono, Nordin N, Liew KH, et al. Fluorine-doped tin oxide catalyst for glycerol conversion to methanol in sub-critical water. *J Supercrit Fluids* 2017;120:366–78.
- [50] Shan JJ, Lucci FR, Liu J, El-Soda M, Marcinkowski MD, Allard LF, et al. Water co-catalyzed selective dehydrogenation of methanol to formaldehyde and hydrogen. *Surf Sci* 2016;650:121–9.
- [51] García-García FR, Tsang SC, Li K. Hollow fibre based reactors for an enhanced H₂ production by methanol steam reforming. *J Membrane Sci* 2014;455:92–102.